

# On the viscous modes of instability of a trailing line vortex

By MEHDI R. KHORRAMI†

Department of Mechanical Engineering and Mechanics, Old Dominion University,  
Norfolk, VA 23529-0247, USA

(Received 8 January 1990 and in revised form 24 August 1990)

A viscous linear stability analysis of a trailing line (Batchelor) vortex is presented. Employing a staggered Chebyshev spectral collocation technique, very accurate results were obtained. The destabilising role of viscous forces has been shown to produce two types of viscous instability modes. These viscous disturbances consist of an axisymmetric mode and an asymmetric mode. Both disturbances are long-wave instabilities with maximum growth rates which are orders of magnitude smaller than the inviscid modes which have been found by others. Comparison with experimental results and condensation trail observations are found to be in good qualitative agreement with the present study.

---

## 1. Introduction

The hazard associated with the trailing line vortices generated by large commercial jetliners and its effect in reducing the flight frequencies at major airports has been known for many years. To date no satisfactory solution has evolved. With the projected growth in passenger traffic, this limit will result in flight delays and prohibit revenue growth. These considerations have brought the task of manipulation and control of trailing line vortices into the forefront of active research.

This study is concerned mainly with a viscous stability analysis of an isolated trailing line vortex. The motivation for undertaking such analysis is twofold. First, except for the work of Lessen & Paillet (1974) and Stewartson (1982), there are no other viscous stability calculations for trailing line vortices. Since Lessen & Paillet's work was limited to low Reynolds numbers ( $Re \lesssim 150$ ), which will be shown later to be inadequate, questions concerning more realistic flow conditions remain, while the asymptotic analysis of Stewartson cannot be applied directly to disturbances with low azimuthal wavenumbers. Secondly, the recent study of Khorrami, Malik & Ash (1989) showed substantial quantitative disagreement with the results of Lessen & Paillet. In a detailed study, Khorrami (1989) showed that the discrepancy was caused primarily by the small radius of integration employed by Lessen & Paillet.

Much effort in the past has been directed toward understanding the stability characteristics of a trailing line vortex. Subjecting a Batchelor vortex to inviscid disturbances, Duck & Foster (1980) found a continuous spectrum of unstable modes. The spectrum contained infinite numbers of higher modes for each combination of axial wavenumber,  $\alpha$ , azimuthal wavenumber,  $n$ , and swirl parameter,  $q$ , where their

† Present address: High Technology Corporation, 28 Research Drive, Hampton, VA 23666, USA.

calculated primary mode corresponded to the mode obtained by Lessen, Singh & Paillet (1974). The findings of Duck & Foster have since been confirmed by many other researchers, notably the asymptotic analysis of Leibovich & Stewartson (1983), Stewartson & Capell (1985), Stewartson & Brown (1985), Duck (1986), and Stewartson & Leibovich (1987). Recently, it was shown by Khorrami *et al.* (1989) that, although the higher modes are inviscid by nature, they persist to much lower Reynolds numbers. The extensive inviscid studies of Ito, Suematsu & Hayase (1985), Foster & Duck (1982) and Staley & Gall (1984) suggest that this is an inherent feature of swirling flows. These inviscid disturbances have large growth rates and very short e-folding times as compared to conventional boundary-layer instabilities. Although the maximum growth rate increases with  $n$ , Leibovich & Stewartson (1983) have shown that this maximum asymptotes to a value,  $\omega_{i\infty}$ , as  $n$  becomes very large. It seems that the large growth rates of the inviscid modes with negative azimuthal wavenumbers and their complex structure have drawn the attention of most researchers in recent years, at the expense of any viscous analysis. The prevailing opinion in the stability community has been that the role of viscosity is a stabilising one. However, the asymptotic analysis of Maslowe & Stewartson (1982) indicated that the role of viscosity in swirling flows is more subtle than thought previously, and that it alters the shape of the perturbation eigenfunctions significantly. The discovery of two viscous modes of instability in this study confirms their suspicions and demonstrates the destabilising influence of viscosity. The viscous disturbances reported here are for azimuthal wavenumbers which (for the case of the Batchelor vortex) have never been reported to be unstable. These new instabilities are presented in detail in §4.2.

## 2. Stability formulation

Cylindrical-polar coordinates  $(r, \theta, z)$  are chosen as the coordinate system. Following Lessen *et al.* (1974), the far-wake solution for a trailing line vortex due to Batchelor (1964) is of the form

$$U = 0, \quad V = \frac{q}{r}(1 - e^{-r^2}), \quad W = \frac{W_1}{W_2} + e^{-r^2}, \quad (2.1)$$

where  $U$ ,  $V$  and  $W$  are the radial, tangential and axial velocities, respectively. The swirl parameter,  $q$ , is related to the ratio of the maximum swirl velocity to the maximum axial velocity excess (or defect). The flow variables are decomposed into a mean part and an infinitesimally small perturbation, i.e.

$$\tilde{u} = U + u, \quad \tilde{v} = V + v, \quad \tilde{w} = W + w, \quad \tilde{p} = \Pi + p. \quad (2.2)$$

Employing normal mode analysis, the above perturbations are Fourier decomposed and assumed to be of the form

$$\{u, v, w, p\} = \{iF(r), G(r), H(r), P(r)\} e^{i(\alpha z + n\theta - \omega t)}, \quad (2.3)$$

where  $F$ ,  $G$ ,  $H$  and  $P$  are the complex disturbance eigenfunctions,  $\alpha$  is the axial wavenumber,  $n$  is the azimuthal wavenumber, being either zero or an integer, and  $\omega$  is the frequency. For any temporal solution,  $\alpha$  is real and  $\omega$  is complex.

The linearized form of the equations of motion for steady flow of an incompressible fluid, in terms of perturbation eigenfunctions, were obtained by Lessen & Paillet (1974) and can be written

$$\text{continuity:} \quad F' + \frac{F}{r} + \frac{nG}{r} + \alpha H = 0, \quad (2.4)$$

$r$ -momentum:

$$\begin{aligned} -\frac{iF''}{Re} + i \left[ U - \frac{1}{Re r} \right] F' + \left[ \omega + i \frac{dU}{dr} - \frac{nV}{r} - \alpha W \right. \\ \left. + \frac{i}{Re} \left( \frac{n^2 + 1}{r^2} + \alpha^2 \right) \right] F + \left[ \frac{i2n}{Re r^2} - \frac{2V}{r} \right] G + P' = 0, \end{aligned} \quad (2.5)$$

$\theta$ -momentum:

$$\begin{aligned} -\frac{G''}{Re} + \left[ U - \frac{1}{Re r} \right] G' + \left[ -i\omega + \frac{inV}{r} + i\alpha W + \frac{U}{r} \right. \\ \left. + \frac{1}{Re} \left( \frac{n^2 + 1}{r^2} + \alpha^2 \right) \right] G + \left[ i \frac{dV}{dr} + \frac{2n}{Re r^2} + \frac{iV}{r} \right] F + \frac{inP}{r} = 0, \end{aligned} \quad (2.6)$$

$z$ -momentum:

$$-\frac{H''}{Re} + \left[ U - \frac{1}{Re r} \right] H' + \left[ -i\omega + \frac{inV}{r} + i\alpha W + \frac{1}{Re} \left( \frac{n^2 + \alpha^2}{r^2} \right) \right] H + i \frac{dW}{dr} F + i\alpha P = 0, \quad (2.7)$$

where primes denote differentiation with respect to the radial coordinate. The non-dimensionalization is done with respect to the viscous core radius and the centreline axial velocity deficit or excess as defined by Lessen *et al.* (1974), and  $Re$  is the Reynolds number based on the core radius and velocity excess.

This set of governing equations must satisfy six boundary conditions. At a large distance from the centreline the three components of the velocity are zero. That is

$$F(\infty) = G(\infty) = H(\infty) = 0. \quad (2.8)$$

At the axis of the vortex,  $r = 0$ , the solutions are required to be smooth and single valued. The conditions on the centreline are dependent on the value of the azimuthal wavenumber  $n$  and are given by Batchelor & Gill (1962) as

$$\text{if } n = 0, \quad F(0) = G(0) = 0, \quad H'(0) = 0, \quad (2.9)$$

$$\text{if } n = \pm 1, \quad F(0) \pm G(0) = 0, \quad F'(0) = 0, \quad H(0) = 0, \quad (2.10)$$

$$\text{or if } |n| > 1, \quad F(0) = G(0) = H(0) = 0. \quad (2.11)$$

### 3. Numerical method

A staggered Chebyshev spectral collocation method was employed in the numerical calculations. The merits of choosing the collocation method and how it is implemented are explained at some length by Khorrami *et al.* (1989) and Khorrami (1991). Consequently, only a brief outline of the technique is presented here. In this method (see Gottlieb & Orszag 1977 and Gottlieb, Hussaini & Orszag 1984), the perturbation eigenfunctions are expanded in terms of a truncated Chebyshev series, i.e.

$$F(\xi) = \sum_{k=0}^N a_k T_k(\xi), \quad (3.1)$$

where  $\xi$  is the independent variable in Chebyshev space. Next, the governing

equations (2.4)–(2.7) are discretized so that the velocities and the three momentum equations are evaluated at the grid points while pressure and the continuity equation are enforced at the mid grid points. For this staggered grid, the velocities are evaluated at the collocation points  $\xi_j$  which are the extrema of the last retained Chebyshev polynomial ( $T_N(\xi)$ ) in the truncated series, while the pressure and the continuity equation are evaluated at the collocation points  $\xi_{j+1/2}$  which are the roots of  $T_N(\xi)$ . The physical domain  $[0, r_{\max}]$  is mapped into the Chebyshev space  $[-1, 1]$  via an algebraic transformation. The accuracy and convergence of the solution and its dependence on the value of  $r_{\max}$ , where the far-field boundary conditions are imposed, were tested extensively. A detailed study reported by Khorrami *et al.* (1989) showed that  $r_{\max} = 100$  was sufficient and the number of required Chebyshev polynomials,  $N$ , varied between 50 and 70, depending on flow Reynolds number.

The discretised equations of motion plus the six boundary conditions for velocities constitute a generalised eigenvalue system for the complex eigenvalue  $\omega$ . The general complex eigenvalue solver employed in the global calculations is the IMSL QZ routine called EIGZC. If the eigenfunctions are desired, the eigenvalues are refined and the eigenfunctions are obtained subsequently using a local method. The local method which was employed here uses an inverse iterative technique (see Wilkinson 1965). The discretisation of the governing equations for the local method is spectral but non-staggered. It was found that the eigenvalues obtained by the local procedure always converged to eight or nine significant digits within four iterations. Furthermore, it was found that both methods produced eigenvalues which were in agreement up to at least six-digit accuracy.

## 4. Results and discussion

The quantity  $W_1/W_2$  in equation (2.1) represents the uniform outer flow and throughout the present study it is assumed that  $W_1/W_2 = 1$ . It has been pointed out by Lessen *et al.* (1974) that the translation or inversion of the axial velocity affects the frequency only while the growth rate,  $\omega_i$ , remains unchanged. This is correct but it should also be noted that inversion of the axial velocity profile causes the sign of the unstable azimuthal wavenumber,  $n$ , to change. This feature has physical significance, since waves with negative  $n$  have different orientation with respect to the rotating flow than those with positive values.

### 4.1. Inviscid instabilities

First, as a test case, the variation with axial wavenumber,  $\alpha$ , of the growth rate of the unstable modes for  $n = -2$  and  $q = 0.8$ , at a Reynolds number of 10000 were computed. The curves were identical to the ones obtained from the inviscid calculations of Duck & Foster (1980). It is logical then to assume that the instability is an inviscid one. The variation of the real part of the frequency,  $\omega_r$ , with  $\alpha$  associated with these higher modes showed similar trends and were nearly identical to the corresponding curve for the primary mode. This strange behaviour, which was first shown to exist via the asymptotic analysis of Leibovich & Stewartson (1983), seems to be a feature of the inviscid modes. The calculations for the case of  $n = -1$  at  $Re = 10\,000$ ,  $q = 0.4$  showed similar behaviour to that of the  $n = -2$  mode. Again, the results matched exactly with Duck & Foster (1980) while the primary mode corresponded to the inviscid mode obtained by Lessen *et al.* (1974). The variation of the first two modes with Reynolds number for the case of  $n = -2$  at two distinct values of  $\alpha$  and  $q = 0.8$  are shown in figures 1 and 2. The inviscid nature of these

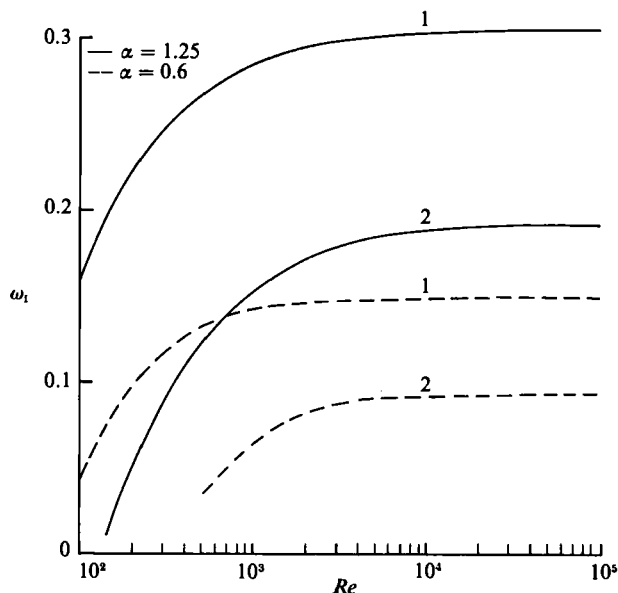


FIGURE 1. Variation of the growth rate of  $n = -2$  disturbances with Reynolds number ( $q = 0.8$ ).

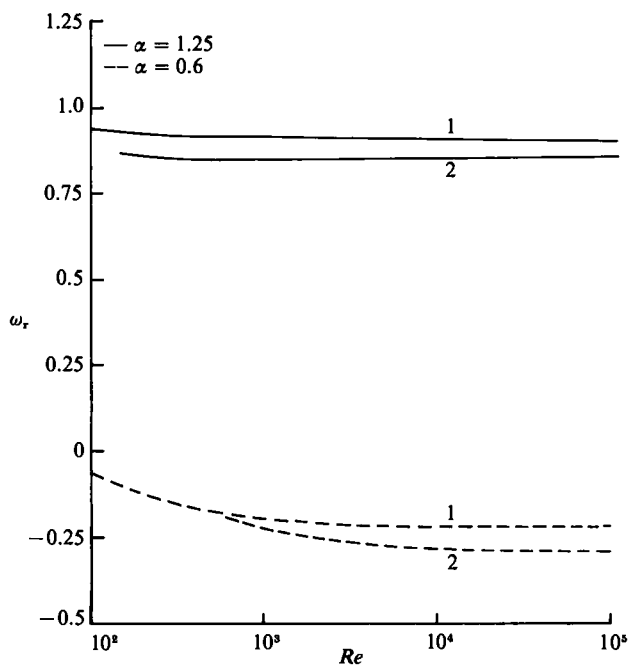


FIGURE 2. Variation of the real part of frequency of  $n = -2$  disturbances with Reynolds number ( $q = 0.8$ ).

modes is self-evident from these plots. It is clear that for Reynolds numbers as low as 10000, these modes have almost attained their maximum growth rates and are virtually independent of  $Re$ . Although not displayed here, similar behaviour exists for the case of  $n = -1$  and other higher negative azimuthal wavenumbers.

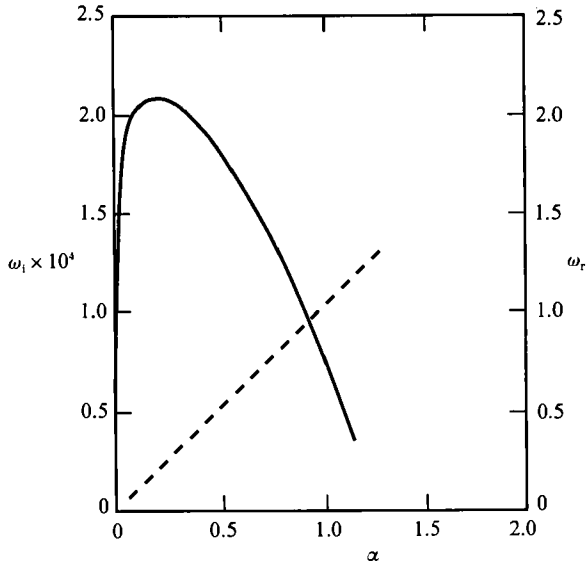


FIGURE 3. Variation of the frequency of axisymmetric ( $n = 0$ ) disturbances with wavenumber for  $q = 1.0$ ,  $Re = 10^4$ . Solid line:  $\omega_i$ , broken line:  $\omega_r$ .

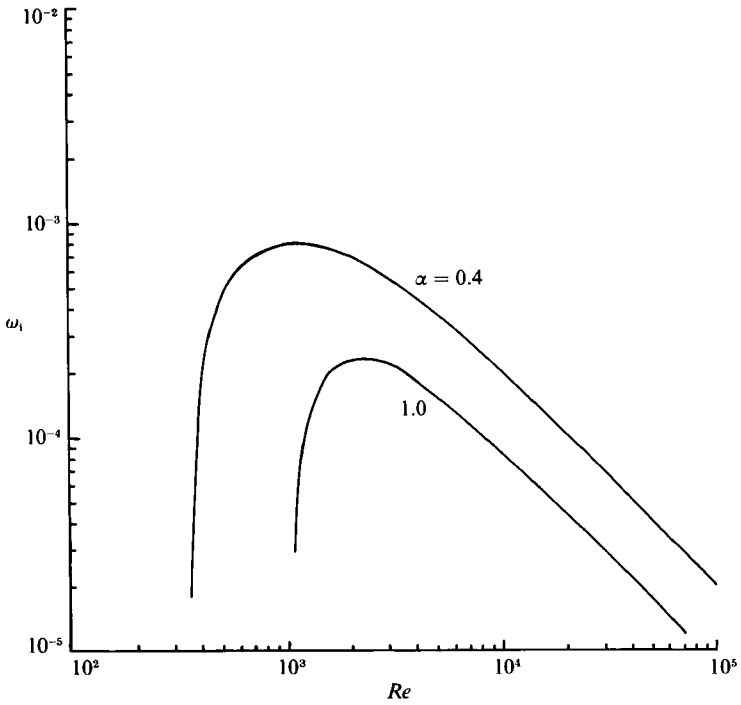


FIGURE 4. Variation of the growth rate of axisymmetric ( $n = 0$ ) disturbances with Reynolds number for  $q = 1.0$ .

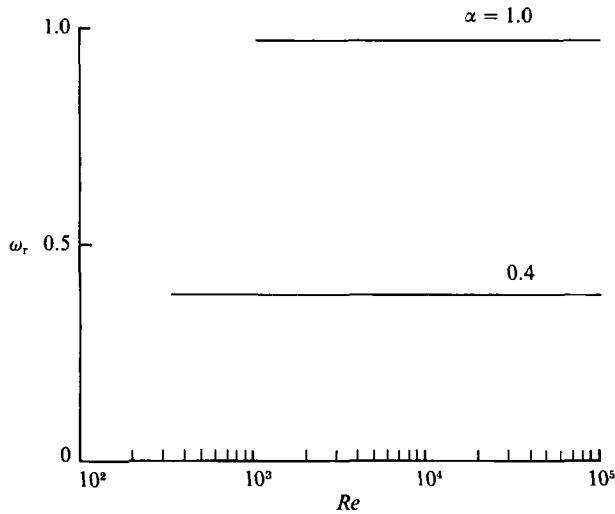


FIGURE 5. Variation of the real part of the frequency of axisymmetric ( $n = 0$ ) disturbances with Reynolds number for  $q = 1.0$ .

#### 4.2. Viscous instabilities

The two viscous instabilities discovered in this study correspond to an axisymmetric,  $n = 0$ , mode and an asymmetric,  $n = 1$ , mode. Figure 3 shows the variation of  $\omega$  with  $\alpha$  for  $n = 0$ ,  $q = 1$  and  $Re = 10000$ . The figure indicates that this instability has a growth rate which is orders of magnitude smaller than the inviscid modes. The maximum value of  $\omega_i$  occurs at  $\alpha \approx 0.3$  which suggests that the disturbance wavelength is on the order of the core radius of the vortex. Overall it is safe to say that this is a long-wave instability. The variation of the real part of the frequency with  $\alpha$  shows an almost linear behaviour, which indicates that the axial phase speed of the wave,  $c_r = \omega_r/\alpha$ , is constant and nearly equal to unity over a wide range of  $\alpha$ . This fact suggests that the disturbance is travelling with the same speed as the constant outer velocity field. Variation of  $\omega$  with Reynolds number is presented in figures 4 and 5, for two distinct wavenumbers. The viscous nature of the axisymmetric mode is shown clearly in figure 4. As the Reynolds number increases, the disturbance attains its maximum growth rate very rapidly and then drops gradually. The maximum of  $\omega_i$  shifts to higher  $Re$  as  $\alpha$  increases and there is a significant drop in its magnitude. Figure 5 shows that the phase speed is constant over a wide range of Reynolds numbers and has a magnitude which is slightly less than the uniform outer flow. The variation of the wavenumber of the maximum growth rate with Reynolds number is shown in figure 6. The curve is consistent with the behaviour of a viscous mode and shows the damping effect of viscosity on the wavenumber at moderate Reynolds numbers. The effect of swirl parameter,  $q$ , on the growth rate for  $\alpha = 0.4$  is displayed in figure 7. As the Reynolds number increases, the range of  $q$  where instability exists also increases while the position where  $\omega_i$  reaches its maximum shifts to lower values of the swirl parameter. It is apparent from this figure that the increase in the range of  $q$  only takes place with respect to lower values of  $q$  while all three curves asymptote to  $q \approx 1.26$  for higher values, where the instability disappears.

Owing to the small growth rate and high Reynolds number associated with these viscous modes, care must be taken to ensure that the results are fully converged. The

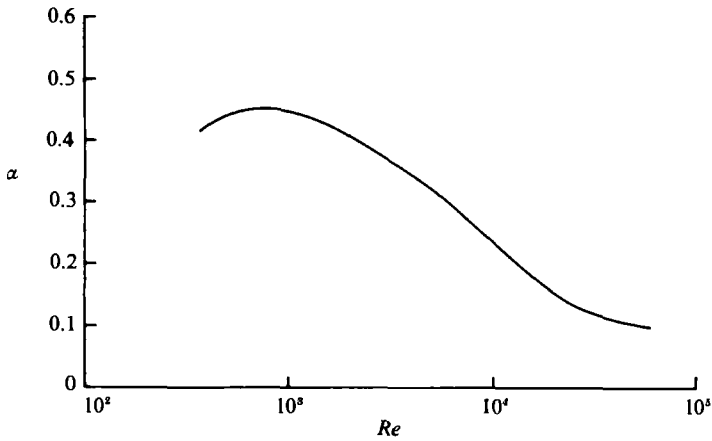


FIGURE 6. Influence of Reynolds number on the variation of the axial wavenumber associated with the maximum growth rate of axisymmetric ( $n = 0$ ) disturbances, when  $q = 1.0$ .

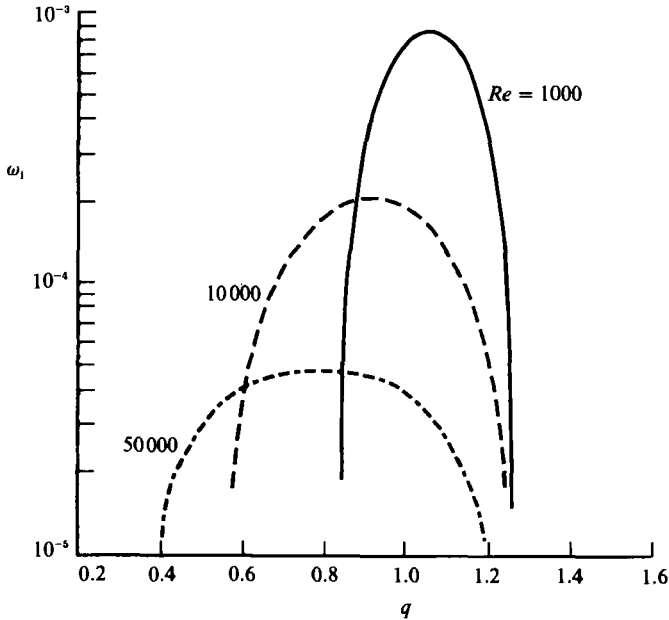


FIGURE 7. Variation of the growth rate of axisymmetric ( $n = 0$ ) disturbances with swirl parameter for  $\alpha = 0.4$ .

Chebyshev spectral collocation method is well suited to such flows since, with a relatively small number of polynomials, very accurate eigenvalues are computed. The convergence behaviour of the axisymmetric ( $n = 0$ ) viscous mode at  $Re = 10000$  is presented in table 1. The table shows that five- or six-digit accuracy is easily obtained. Finally, although the global method employed in this study is not suitable to calculate critical values, the interest in this axisymmetric mode justified the effort. The critical values are compiled for the different control parameters for this mode in table 2. The critical Reynolds number,  $Re_c$ , given in this table is the lowest Reynolds



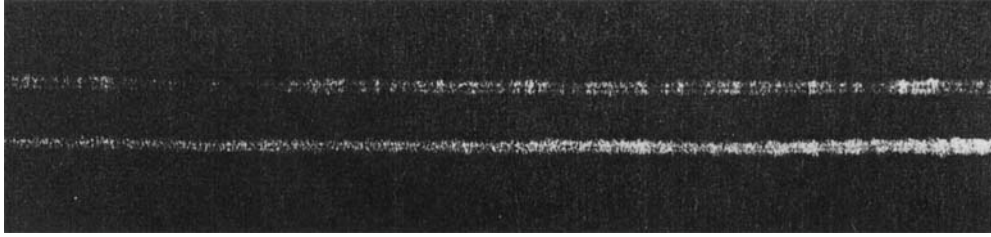


FIGURE 8. Photographic evidence of the growth of axisymmetric ( $n = 0$ ) disturbances in the upper trail of an aircraft contrail (from Bisgood 1980).

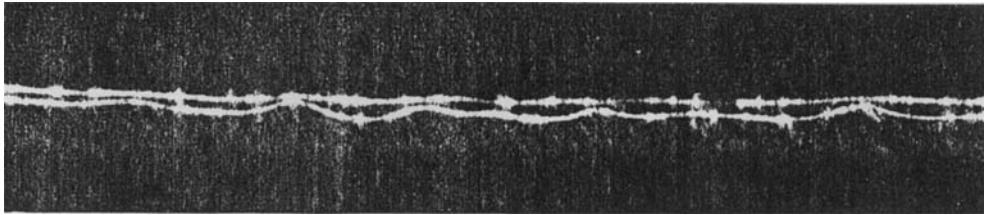


FIGURE 9. Photographic record of the amplification of axisymmetric ( $n = 0$ ) waves on an aircraft contrail (from Bisgood 1980).

---

$N$	$\omega$
36	$0.483\,592\,892 + i0.000\,184\,796\,2$
42	$0.483\,592\,862 + i0.000\,184\,803\,7$
46	$0.483\,592\,828 + i0.000\,184\,686\,7$
50	$0.483\,592\,832 + i0.000\,184\,685\,3$

TABLE 1. The convergence behaviour of axisymmetric ( $n = 0$ ) viscous mode with the number of Chebyshev polynomials,  $N$ . Here,  $\alpha = 0.5$ ,  $Re = 10000$ , and  $q = 1.0$

---

$\alpha_c$	$Re_c$	$q_c$	$\omega$
0.468	322.35	1.08	$0.441\,679 - i4.97 \times 10^{-7}$

TABLE 2. Critical values of different parameters for the axisymmetric case  $n = 0$

---

number, together with the corresponding  $q$  and  $\alpha$  for which the instability first occurred.

There is a phenomenon closely resembling the axisymmetric mode just described which has been observed in experiments and photographs of many condensation trails from commercial aircraft. Although the phenomenon is termed 'core bulging' or 'core bursting' in the literature, the present author believes that is a misnomer since it appears to be travelling outside the core and the core remains intact. It is only in the later stages that the growth of these disturbances affect the core structure. This fact is demonstrated in the photographs shown in figures 8–10. These photographs, which are contrails from a large commercial aircraft, were reproduced from the work of Bisgood (1980). They were taken from the ground with the vortices at heights between 10000 and 12000 m. The separation distance between the vortices

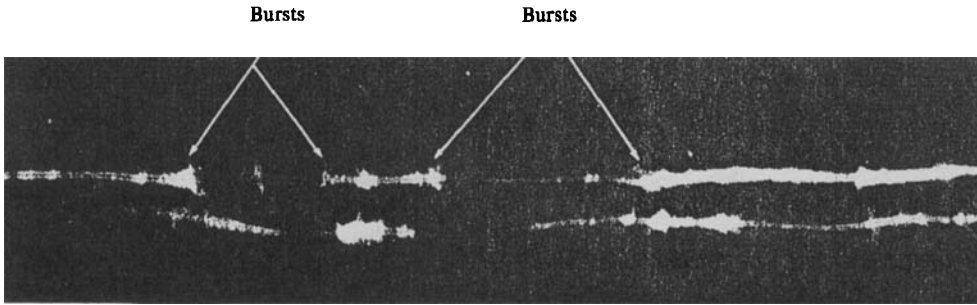


FIGURE 10. Further growth and bursting of axisymmetric ( $n = 0$ ) wave forms on contrails (from Bisgood 1980).

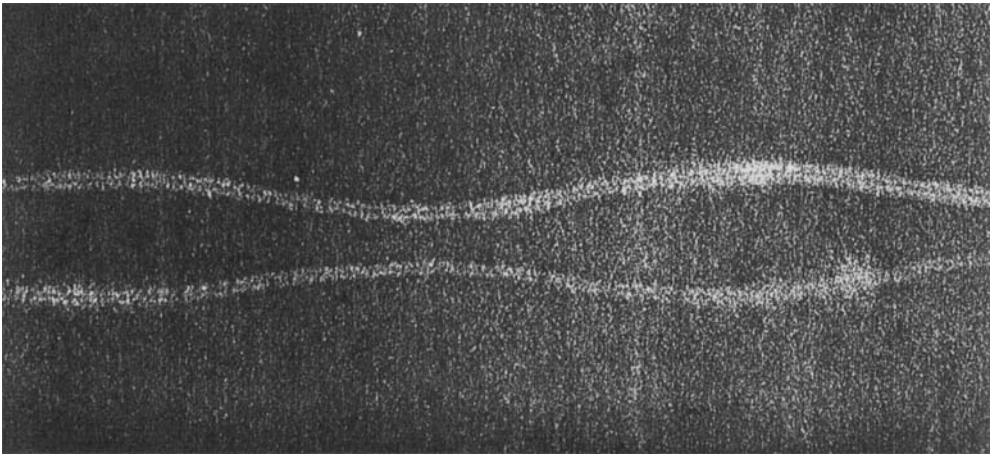


FIGURE 11. Crow's classical 'sinuosities' mode (from Bisgood 1980).

was between 25 and 40 m. Figure 8 show that while axisymmetric disturbances are present (Bisgood has called it the 'dotting' effect), the core still remains intact. The next two photos (figures 9 and 10) show the amplification and growth of these waves. It must be emphasized here that these photographs are not sequential and might not even be the same contrails. However, the presence of the inductive instability (Crow 1970) due to the vortex pair should also be noted in figures 9 and 10. The case of Crow instability is mentioned here merely to emphasize that the existence of these two forms of instability (core bulging and Crow) does not depend upon the simultaneous presence of both and they do not appear to interact significantly. This conclusion was established recently by Sarpkaya (1983) and Sarpkaya & Daly (1987) who found that any combination of the instabilities might occur. A simple calculation for the maximum growth rate obtained in this study revealed that the axisymmetric mode has an e-folding time very close to that of the Crow instability. Figures 9 and 10 lend support to such a conjecture.

Figure 11 is another photograph which has been reproduced from the work of Bisgood (1980). Sarpkaya's findings can be supported by this picture which shows Crow's classical 'sinuosities' mode without any sign of the axisymmetric wave form. Until additional research is carried out, further comments on the nature of the

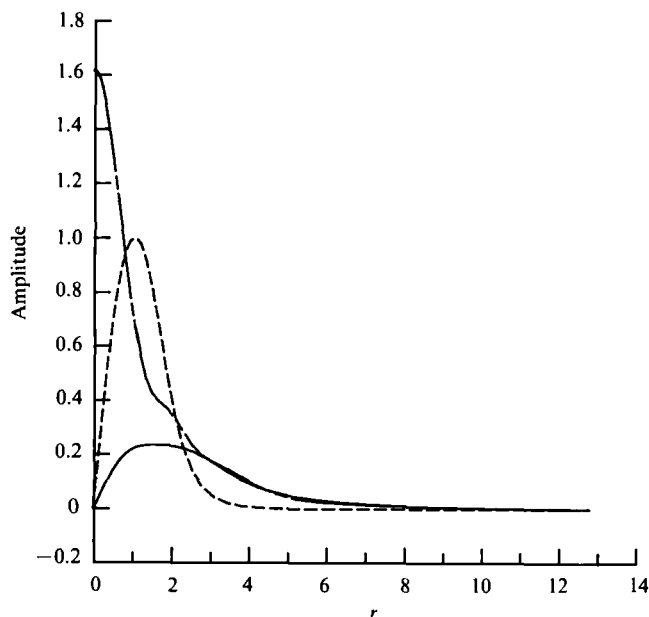


FIGURE 12. Spatial distribution of the amplitude of various eigenfunction components of an axisymmetric ( $n = 0$ ) perturbation: —, radial velocity; ---, azimuthal velocity; — · —, axial velocity. Here,  $\alpha = 0.4$ ,  $q = 1.0$ , and  $Re = 400$ .

interaction between these two distinct forms of instabilities are speculative and therefore unjustified. It may be presumptuous to state that a Batchelor vortex is a good approximation in studies of aircraft trailing line vortex stability because of questions concerning laminar and turbulent effects. However, the similarity between contrail observations and the present predictions is relevant. Crow & Champaign (1971) found that local large-scale motions in axisymmetric jets could be traced back to linearly unstable modes regardless of whether the jet was laminar or turbulent. A similar conclusion was drawn for other forms of free shear layers by several other researchers (see Ho & Huerre 1984). Apparently, the present linear calculations which seem to capture (at least qualitatively) some of the local large-scale phenomena point to the possibility of similar conjectures for the case of a trailing line vortex.

The core radius where the azimuthal mean velocity reaches its maximum is at approximately  $r = 1.1$ . In order to substantiate the fact that the axisymmetric wave is occurring and that it spreads beyond the core of the vortex, one has to look at the perturbation eigenfunctions. Figure 12 represents the eigenfunction amplitudes of the perturbation components near the critical values. The phase angle plots have been omitted for the sake of space. The eigenfunction amplitudes have been normalised by the maximum amplitude of the azimuthal eigenfunction throughout this study. Figure 12 shows clearly that most of the perturbation energy in the radial and azimuthal directions is spread over a wide distance and is mostly outside of the core. This figure also indicates that the axial perturbation is the dominant component with the maximum amplitude occurring on the centreline. But even in this case a significant portion of the energy lies beyond the core radius. Overall, there is hardly anything happening beyond  $r = 10$ .

The variations of the  $\omega$  with the axial wavenumber,  $\alpha$ , for the asymmetric mode  $n = 1$  are plotted in figure 13 with  $q = 0.4$  and  $Re = 10000$ . This instability has

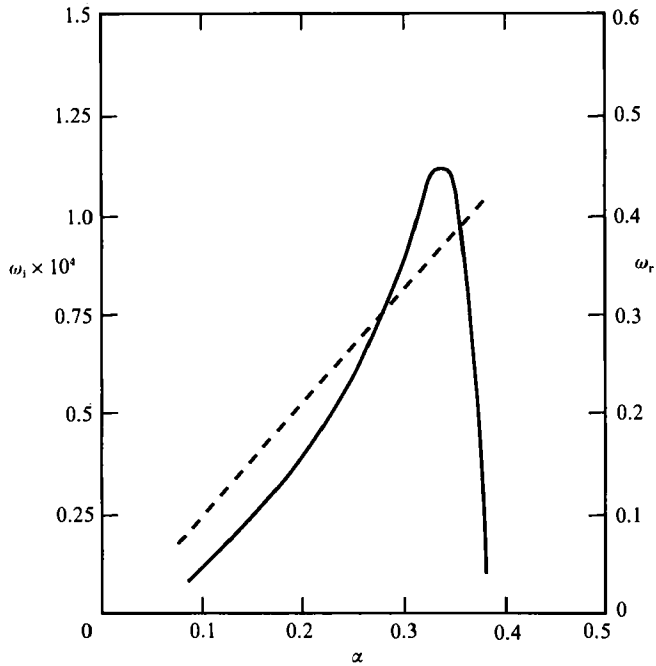


FIGURE 13. Variation of the frequency of asymmetric ( $n = +1$ ) disturbance with wavenumber for  $q = 0.4$ ,  $Re = 10^4$ . Solid line:  $\omega_i$ , broken line:  $\omega_r$ .

---

$N$	$\omega$
44	0.323 455 155 + i0.000 470 672 06
48	0.323 455 110 + i0.000 470 691 49
52	0.323 455 122 + i0.000 470 700 03
56	0.323 455 121 + i0.000 470 697 60
60	0.323 455 121 + i0.000 470 697 69
64	0.323 455 122 + i0.000 470 697 85
66	0.323 455 121 + i0.000 470 697 86

---

TABLE 3. The convergence behaviour of asymmetric ( $n = 1$ ) viscous mode with the number of Chebyshev polynomials,  $N$ . Here,  $\alpha = 0.3$ ,  $Re = 2000$ , and  $q = 0.4$

growth rates which are comparable with the axisymmetric wave but it is unstable over a smaller range of  $\alpha$ . However, like the  $n = 0$  case, it is basically a long-wave instability. The maximum growth rate occurs at  $\alpha \approx 0.34$ . The nearly linear variation of  $\omega_r$  with  $\alpha$  indicates that the axial phase speed of the wave is slightly greater than unity. Like the axisymmetric case, the wave is travelling nominally with the uniform outer mean flow, although it is a bit closer to the core of vortex in this case. The convergence behaviour of the asymmetric viscous mode at  $Re = 2000$  is presented in table 3. The fast convergence associated with the spectral method is also evident in this table.

This form of instability has been observed experimentally both in wind tunnel measurements and contrail photos. The measurements of Singh & Uberoi (1976) and Strange & Harvey (1983) support the existence of an asymmetric disturbance which has an axial wavelength on the order of the core radius. Furthermore, the

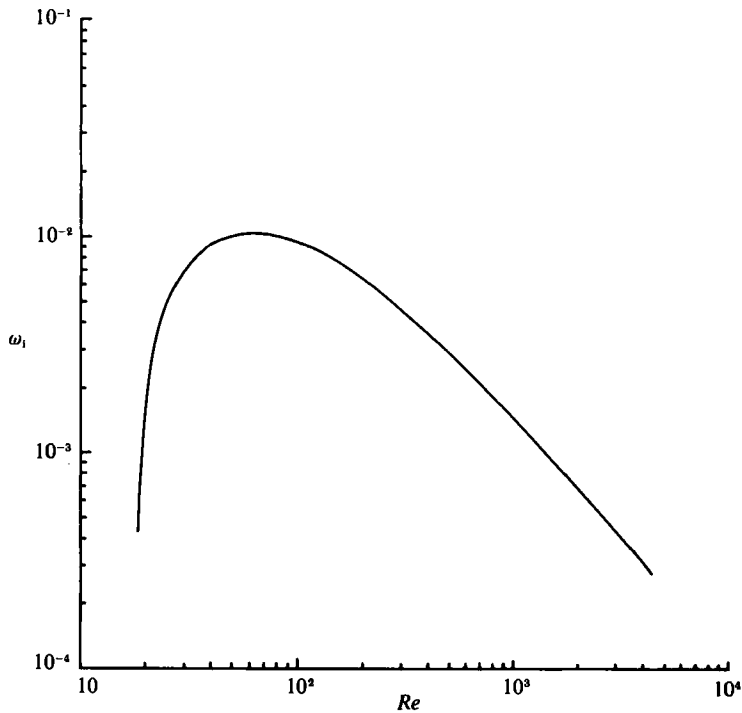


FIGURE 14. Influence of Reynolds number on the growth rate of asymmetric ( $n = +1$ ) disturbances for  $\alpha = 0.34$ ,  $q = 0.4$ .

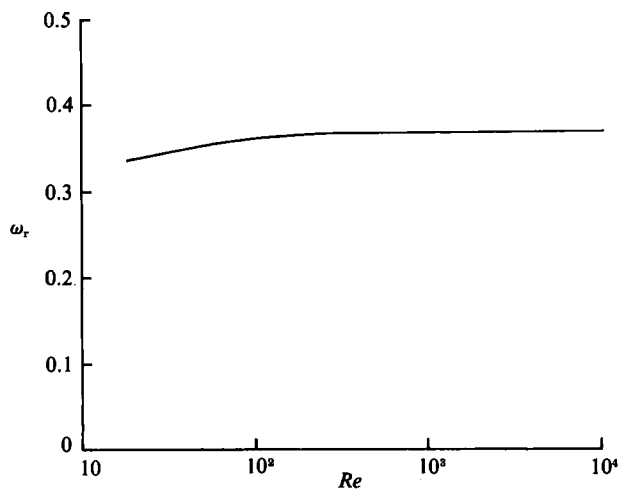


FIGURE 15. Influence of Reynolds number on the real part of the frequency of asymmetric ( $n = +1$ ) disturbances. Here,  $\alpha = 0.34$ ,  $q = 0.4$ .

photograph of condensation trails behind a wide-bodied jet shown in Strange & Harvey (1983) (their figure 1) clearly displays the existence of helical disturbances which coexist with the Crow instability.

The viscous nature of the  $n = 1$  mode is shown in figures 14 and 15. The variation of growth rate  $\omega_1$  with axial wavenumber,  $\alpha$ , shows similar behaviour to that of the

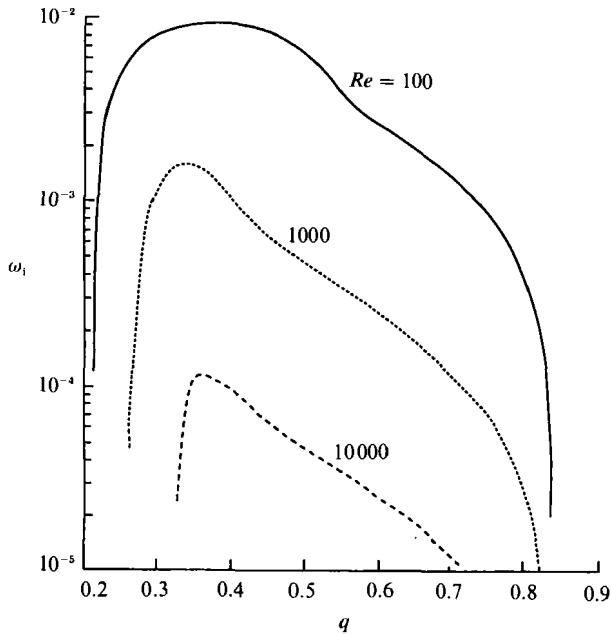


FIGURE 16. Variation of the growth rate of asymmetric ( $n = +1$ ) disturbances with swirl parameter, with  $\alpha = 0.3$ .

$n = 0$  disturbance. However, in this case the instability occurs at lower Reynolds numbers. Also the maximum growth rate which occurs at  $Re \approx 60$  is an order of magnitude greater than the  $\omega_{i\max}$  for the  $n = 0$  mode. But the most interesting phenomenon is the behaviour of these two instabilities at high Reynolds numbers. While the asymmetric mode is the stronger of the two instabilities at low Reynolds numbers, as  $Re$  increases above 10000, the axisymmetric disturbance becomes the mode with the higher growth rate. This may be why, in most of the contrails behind large commercial jets (which occur at high Reynolds numbers), the axisymmetric mode is the dominant and persistent form, while in wind tunnel tests, which are conducted at much lower Reynolds numbers, both modes are present equally. Figure 16 shows the variation of the growth rate of the  $n = 1$  mode with the swirl parameter,  $q$ , for  $\alpha = 0.3$ . Here, unlike the axisymmetric case, as the Reynolds number increases, the range of  $q$  where the instability exists shrinks while the position of maximum growth rate remains fairly stationary. However, similar to the  $n = 0$  mode the higher end of  $q$  for all three curves asymptotes to the same value, in this case  $q \approx 0.83$ .

The amplitudes of the disturbance eigenfunctions are presented in figure 17, which shows that the disturbances having  $|n| = 1$  are the only ones with non-zero radial and azimuthal velocity on the centreline. Although the peaks occur on the centreline, a considerable amount of the perturbation's energy is just outside of the core. Figure 17 also shows the variation of the perturbation amplitude in the axial direction with radial distance. The peak is positioned just inside of the core with a significant part of the perturbation immediately adjacent to the outer part of the core. The overall observation of the eigenfunctions indicates that this instability is narrower in its radial extent than that of the  $n = 0$  disturbance. Although the eigenfunctions were obtained at low Reynolds number, it was found that increases in  $Re$  did not alter the shape of the eigenfunctions significantly. Similar behaviour was observed for the  $n = 0$  mode.

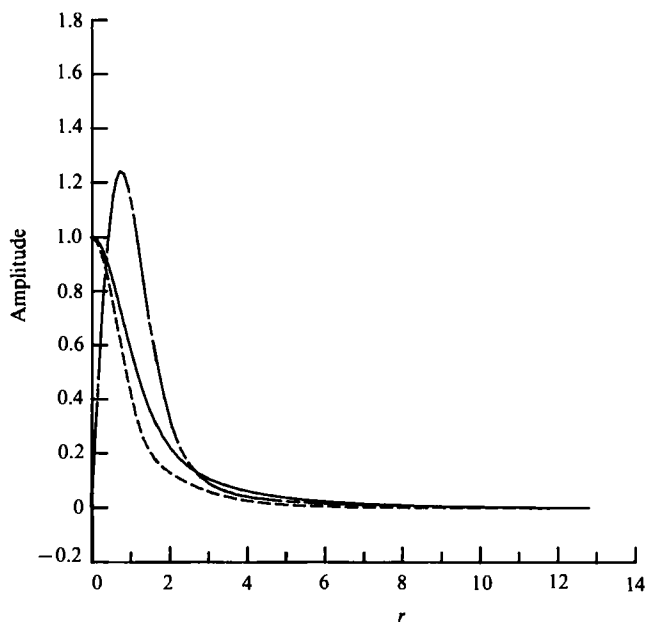


FIGURE 17. Spatial distribution of the amplitude of various eigenfunction components of an asymmetric ( $n = +1$ ) perturbation: —, radial velocity; ---, azimuthal velocity; — · —, axial velocity. Here,  $\alpha = 0.34$ ,  $q = 0.4$  and  $Re = 50$ .

Extensive testing of the  $n = +2$  case and, to a lesser extent,  $n = +3$ , failed to reveal any type of instability – inviscid or viscous. It was found that as the Reynolds number was increased, the flow appeared to approach marginal stability for both  $n = 2$  and 3. Hence, to the extent of these tests, the flow was determined to be unstable only to those perturbations with azimuthal wavenumbers of  $n = 0$  and 1.

Interestingly, unlike inviscid modes, no higher unstable modes were found for either the axisymmetric or asymmetric form of instability. This was tested extensively by going to successively higher values of  $N$  (number of Chebyshev polynomials) than the number needed to obtain convergence. This point has to be explored further. However, since the viscous instabilities occur at finite Reynolds numbers and low azimuthal wavenumbers, a different type of asymptotic expansion is required than that employed for high-wavenumber inviscid modes by previous investigators. Such work is currently in progress and will be reported elsewhere.

## 5. Conclusions

A numerical viscous stability analysis of a trailing line (Batchelor) vortex has been presented. Employing a staggered Chebyshev spectral collocation technique, very accurate results were obtained. The inviscid results of Lessen *et al.* (1974) and Duck & Foster (1980) were confirmed, but it was shown that the higher inviscid modes persist to much lower Reynolds numbers.

The destabilizing nature of viscous forces was revealed by the discovery of two viscous modes of instability. This was the first time that such modes have been shown to exist. These unstable modes consist of an axisymmetric disturbance,  $n = 0$ , and an asymmetric disturbance,  $n = 1$ . Both of these disturbances are found to be fairly long-wave instabilities with an axial wavelength on the order of the vortex core radius. These waves travel along the vortex axis with the uniform outer flow. The

growth rates are found to be orders of magnitude smaller than the inviscid modes. However, comparison with the experimental results of Sarpkaya (1983), Sarpkaya & Daly (1987), Singh & Uberoi (1976), Strange & Harvey (1983) and the condensation trail studies of Bisgood (1980) show such similarity with the viscous predictions that they represent a compelling argument for the existence of these modes.

The author is indebted to Mr Dennis M. Bushnell for his constant support and encouragement and to Professor Robert L. Ash for his helpful comments during the preparation of this paper. Also the critical reviews of the referees are appreciated. This work was supported by NASA Langley Research Center under grant No. NAG-1-530.

#### REFERENCES

- BATCHELOR, G. K. 1964 *J. Fluid Mech.* **20**, 645–658.
- BATCHELOR, G. K. & GILL, A. E. 1962 *J. Fluid Mech.* **14**, 529–552.
- BISGOOD, P. L. 1980 Some observations of condensation trails. *RI Aircraft Establishment TM FS 330*.
- CROW, S. C. 1970 *AIAA J.* **8**, 2172–2179.
- CROW, S. C. & CHAMPAGNE, F. H. 1971 *J. Fluid Mech.* **48**, 547–591.
- DUCK, P. W. 1986 *Z. Angew. Math. Phys.* **37**, 340–360.
- DUCK, P. W. & FOSTER, M. R. 1980 *Z. Angew. Math. Phys.* **31**, 523–530.
- FOSTER, M. R. & DUCK, P. W. 1982 *Phys. Fluids* **25**, 1715–1718.
- GOTTLIEB, D., HUSSAINI, M. Y. & ORSZAG, S. A. 1984 *Theory and applications of spectral methods. In Spectral Methods for Partial Differential Equations* (ed. R. G. Voight, D. Gottlieb & M. Y. Hussaini). Philadelphia: Soc. Indus. & Appl. Maths.
- GOTTLIEB, D. & ORSZAG, S. A. 1977 *Numerical Analysis of Spectral Methods: Theory and Applications*. Philadelphia: Soc. Indus. & Appl. Maths.
- HO, C.-M. & HUERRE, P. 1984 *Ann. Rev. Fluid Mech.* **16**, 365–424.
- ITO, T., SUEMATSU, Y. & HAYASE, T. 1985 *Mem. Faculty of Engng, Nagoya University* **37**, 117–172.
- KHORRAMI, M. R. 1989 A study of the temporal stability of multiple cell vortices. Ph.D. dissertation, Old Dominion University (*NASA Contractor Rep.* 4261).
- KHORRAMI, M. R. 1991 *Intl J. Numer. Methods Fluids* **12** (to appear).
- KHORRAMI, M. R., MALIK, M. R. & ASH, R. L. 1989 *J. Comput. Phys.* **81**, 206–229.
- LEIBOVICH, S. & STEWARTSON, K. 1983 *J. Fluid Mech.* **126**, 335–356.
- LESSEN, M. & PAILLET, F. 1974 *J. Fluid Mech.* **65**, 769–779.
- LESSEN, M., SINGH, P. J. & PAILLET, F. 1974 *J. Fluid Mech.* **63**, 753–763.
- MASLOWE, S. A. & STEWARTSON, K. 1982 *Phys. Fluids* **25**, 1517–1523.
- SARPKAYA, T. 1983 *J. Fluid Mech.* **136**, 85–109.
- SARPKAYA, T. & DALY, J. J. 1987 *AIAA J. Aircraft* **24**, 399–404.
- SINGH, P. I. & UBEROI, M. S. 1976 *Phys. Fluids* **19**, 1858–1863.
- STALEY, D. O. & GALL, R. L. 1984 *J. Atmos. Sci.* **41**, 422–429.
- STEWARTSON, K. 1982 *Phys. Fluids* 1953–1957.
- STEWARTSON, K. & BROWN, S. N. 1985 *J. Fluid Mech.* **156**, 387–399.
- STEWARTSON, K. & CAPELL, K. 1985 *J. Fluid Mech.* **156**, 369–386.
- STEWARTSON, K. & LEIBOVICH, S. 1987 *J. Fluid Mech.* **178**, 549–566.
- STRANGE, C. & HARVEY, J. K. 1983 Instabilities in trailing vortices: flow visualization using hot-wire anemometry. *AGARD-CP-342*.
- WILKINSON, J. H. 1965 *The Algebraic Eigenvalue Problem*. Oxford University Press.